iScience, Volume *23*

Supplemental Information

The Brain Microenvironment Induces DNMT1 Suppression and Indolence of Metastatic Cancer Cells

Eishu Hirata, Kojiro Ishibashi, Shinji Kohsaka, Keiko Shinjo, Shinya Kojima, Yutaka Kondo, Hiroyuki Mano, Seiji Yano, Etsuko Kiyokawa, and Erik Sahai

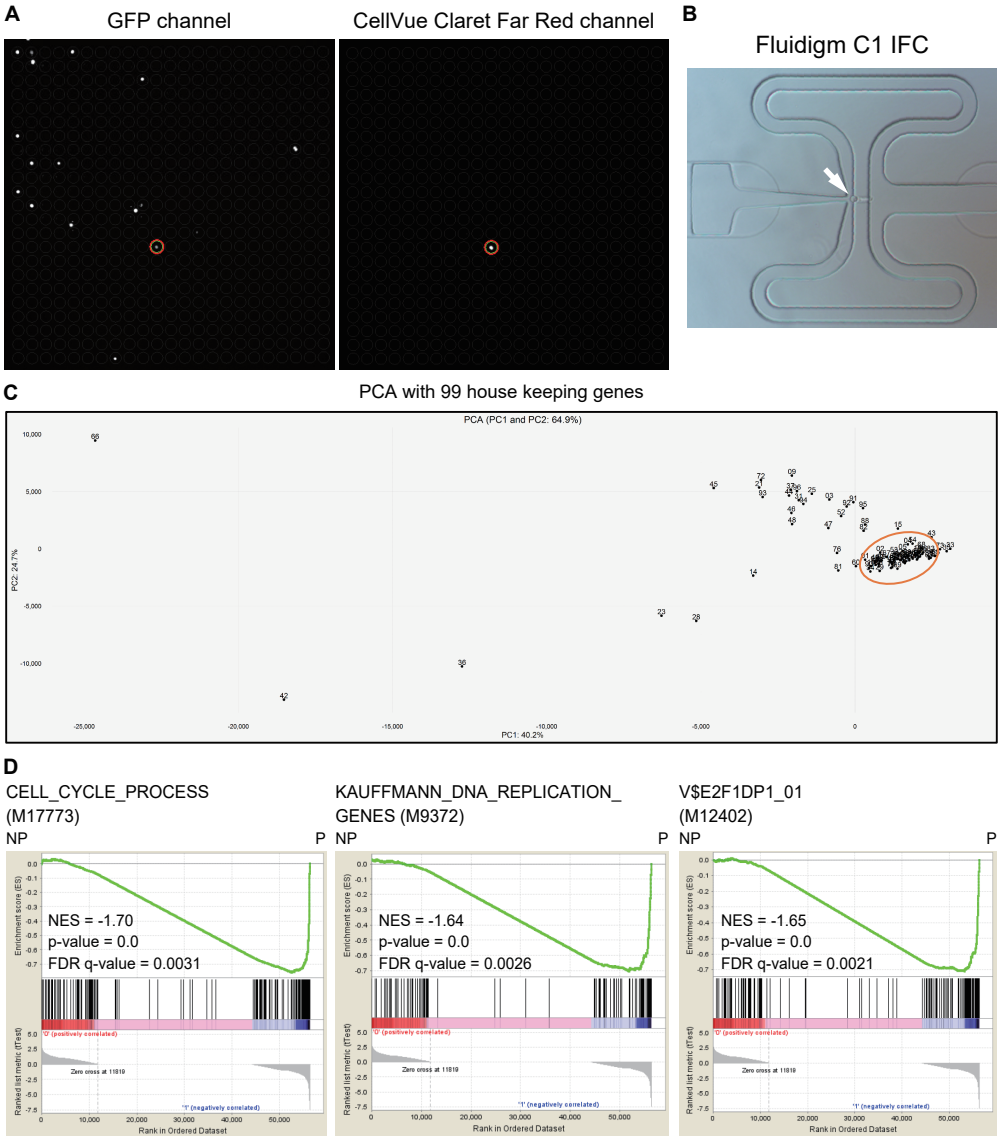

Fig. S1. Hirata et al.

Figure S1 (Related to Figure 1). Collection of brain metastatic WM266.4 cells and preparation of cDNA libraries for single cell RNA sequencing. A, WM266.4-EGFP cells labeled with CellVue Claret Far Red were injected into mouse hearts and induced brain metastasis. WM266.4-EGFP cells were collected from the mouse brains at day 20 and analyzed with ASONE Cell Picking System. The left panel shows GFP channel and the right panel shows the dye channel (CellVue Claret Far Red). A double positive cell is highlighted with a colored circle. Please note that only 16 cells were positive for the dye among 3,077 EGFP-positive cells (positive ratio = 0.52%). **B**, A WM266.4 cell captured on a Fluidigm C1 IFC. **C**, Principal component analysis (PCA) with 99 house-keeping genes selected 61 samples (within an orange circle) as unbiasedly amplified cDNA libraries. **D**, Results of GSEA in Non-proliferating (NP) versus Proliferating (P) group with the indicated gene sets.

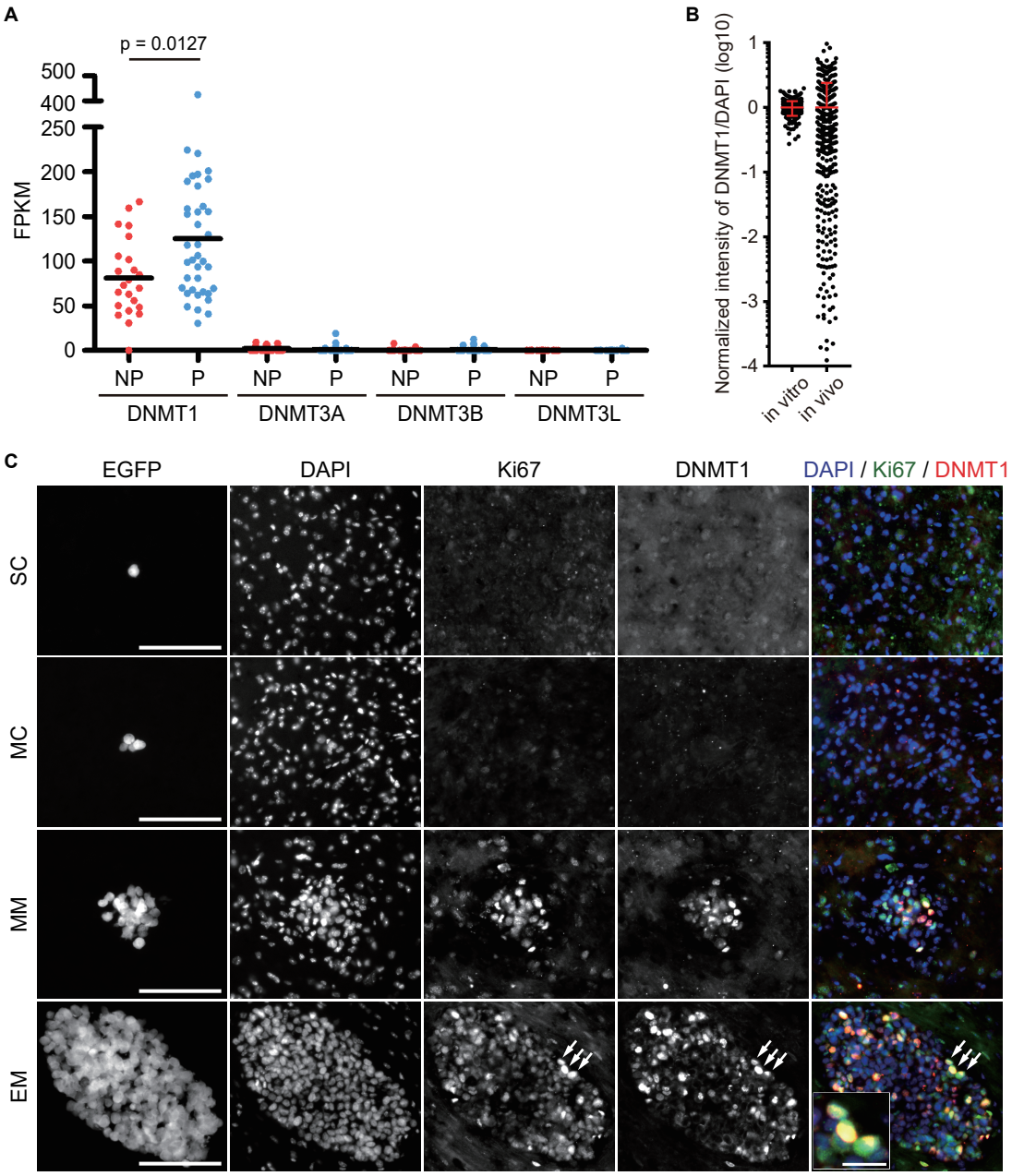

Fig. S2. Hirata et al.

Figure S2 (Related to Figure 2). Ki67 and DNMT1 are co-expressed in brain metastatic WM266.4 cells. A, Expression levels of DNMT family genes in Non-proliferating (NP) and Proliferating (P) group. Bars indicate mean. **B**, Distribution of normalized intensity of DNMT1/DAPI in WM266.4 cells *in vitro* (cultured on a glass bottom dish with DMEM/10% FBS) and *in vivo* (in EM lesions at day 30). 416 cells (*in vitro*) and 350 cells in six EM lesions (*in vivo*) were analyzed. **C**, Representative images of brain metastatic WM266.4 cells double-stained for Ki67 and DNMT1. Arrows indicate representative double-positive cells in EM and enlarged in the small panel. Blue: DAPI, Green: Ki67, Red: DNMT1. Scale = 100 μm (large panels), 20 μm (small panel). Data are mean (**A**) or mean ± s.d (**B**)

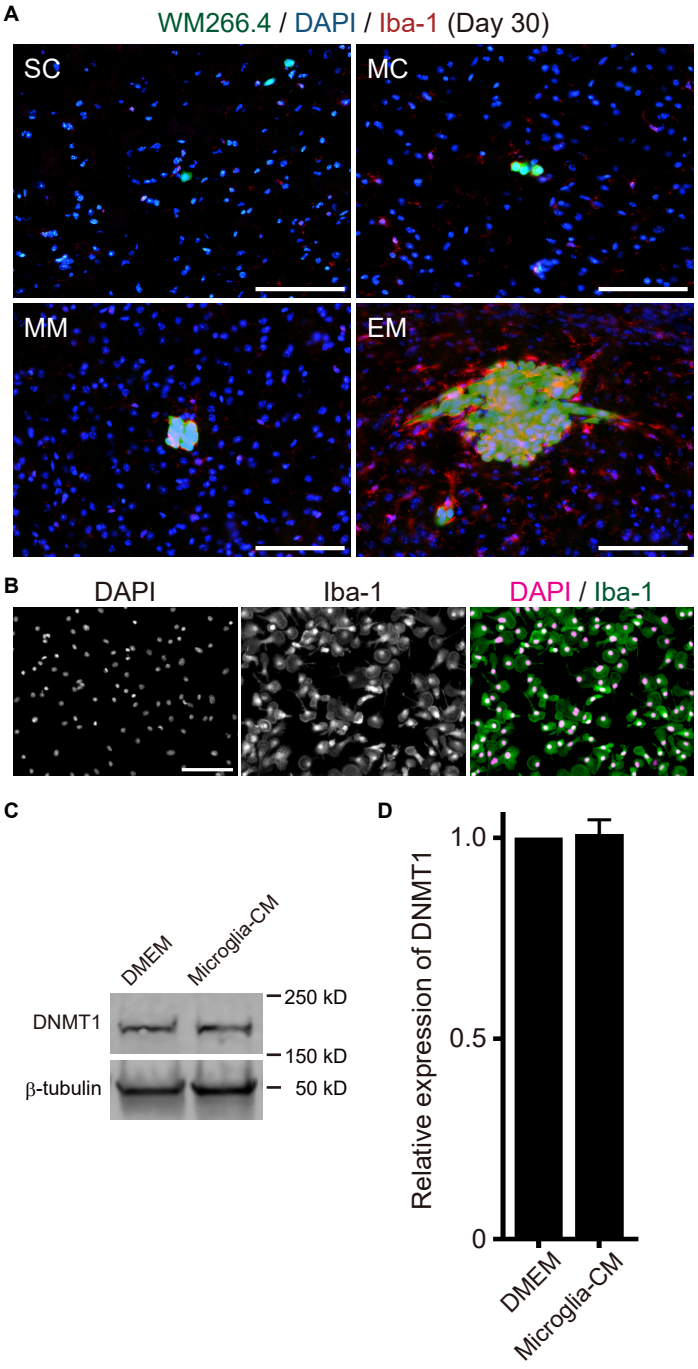

Fig. S3 Hirata et al.

Figure S3 (Related to Figure 4). Conditioned media from cultured microglial cells did not suppress DNMT1 in WM266.4 cells. A, Representative images of brain metastatic WM266.4 cells stained for Iba-1. Green: WM266.4 cells, Blue: DAPI, Red: Iba-1. Scale = 100 μm. **B**, Representative images of primary microglial cells established from C57BL/6 neonatal mouse brains. Cells were stained for Iba-1 and confirmed that more than 90% of the cells were positive for this microglia marker. Green: Iba-1, Magenta: DAPI. Scale = 100 μm. **C** and **D**, Representative images of immunoblotting for DNMT1 in WM266.4 cells cultured in DMEM/10% FBS or conditioned media prepared from microglial cells (**C**) and relative expression of DNMT1/β-tubulin was quantified (**D**) (n = 3). Data are mean ± s.d (D).

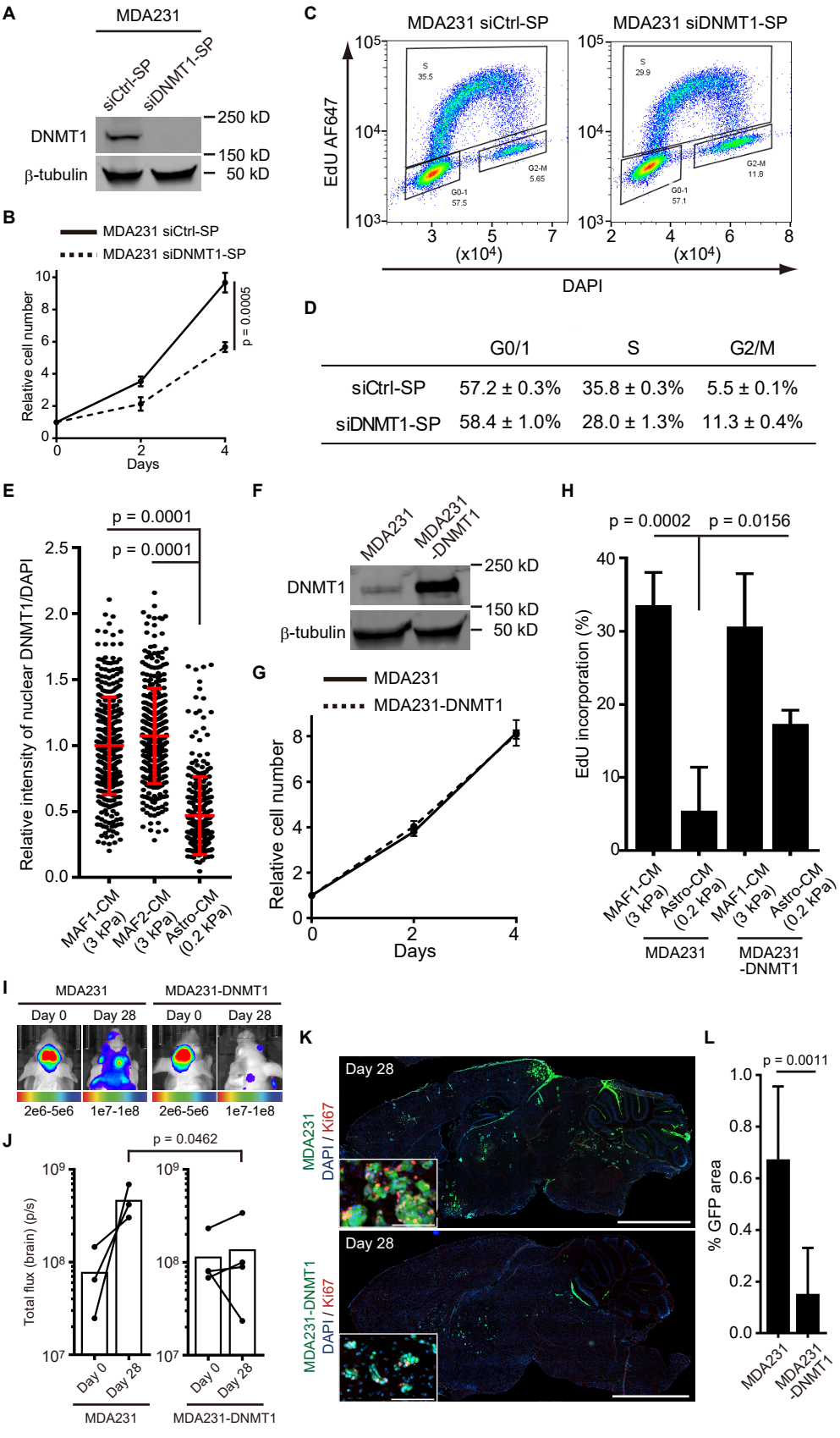

Fig. S4 Hirata et al.

Figure S4 (Related to Figure 3 and 4). DNMT1 suppression induces cell cycle delay in MDA231 human breast cancer cells. A, Immunoblotting at day 7 showed effective ablation of DNMT1 in MDA231 cells treated with siCtrl smart pool (siCtrl-SP) or siDNMT1 smart pool (siDNMT1-SP). **B**, Cell proliferation analysis of MDA231 cells treated with siCtrl-SP or siDNMT1-SP. **C** and **D**, Cell cycle analysis of MDA231 cells treated with siCtrl-SP or siDNMT1-SP with EdU incorporation and DAPI staining (n = 3). **E**, DNMT1 expression in MDA231 cells cultured in the indicated conditions. Y-axis indicates normalized intensity of DNMT1/DAPI (n = 287-359). **F**, Immunoblotting for DNMT1 in MDA231 cells (MDA231) and MDA231 cells overexpressing DNMT1 (MDA231-DNMT1). **G**, Cell proliferation analysis of MDA231 and MDA231-DNMT1 cells (n = 3). **H**, EdU incorporation by MDA231 and MDA231-DNMT1 cells in the indicated culture conditions (n = 6). **I** and **J**, MDA231 or MDA231-DNMT1 cells were injected into mouse hearts and induced brain metastasis. Representative images of bioluminescence detection (**I**) and total flux from brain (**J**) at day 0 (after injection) and day 28 (MDA231; n = 3, MDA231-DNMT1; n = 4) are shown. **K** and **L**, Representative images of sagittal brain sections stained for Ki67 (**K**) and relative tumor areas in the brain sections (% GFP area) at day 28 (**L**) are shown. 6 brain slices from 3 mice (MDA231) and 8 brain slices from 4 mice (MDA231-DNMT1) were used for quantification. Green: MDA-MB-231 cells, Blue: DAPI, Red: Ki67. Scale = 2.5 mm (large images), 100 μm (small panels). Data are mean (**J**) or mean ± s.d (**B**, **D**, **E**, **G**, **H** and **L**).

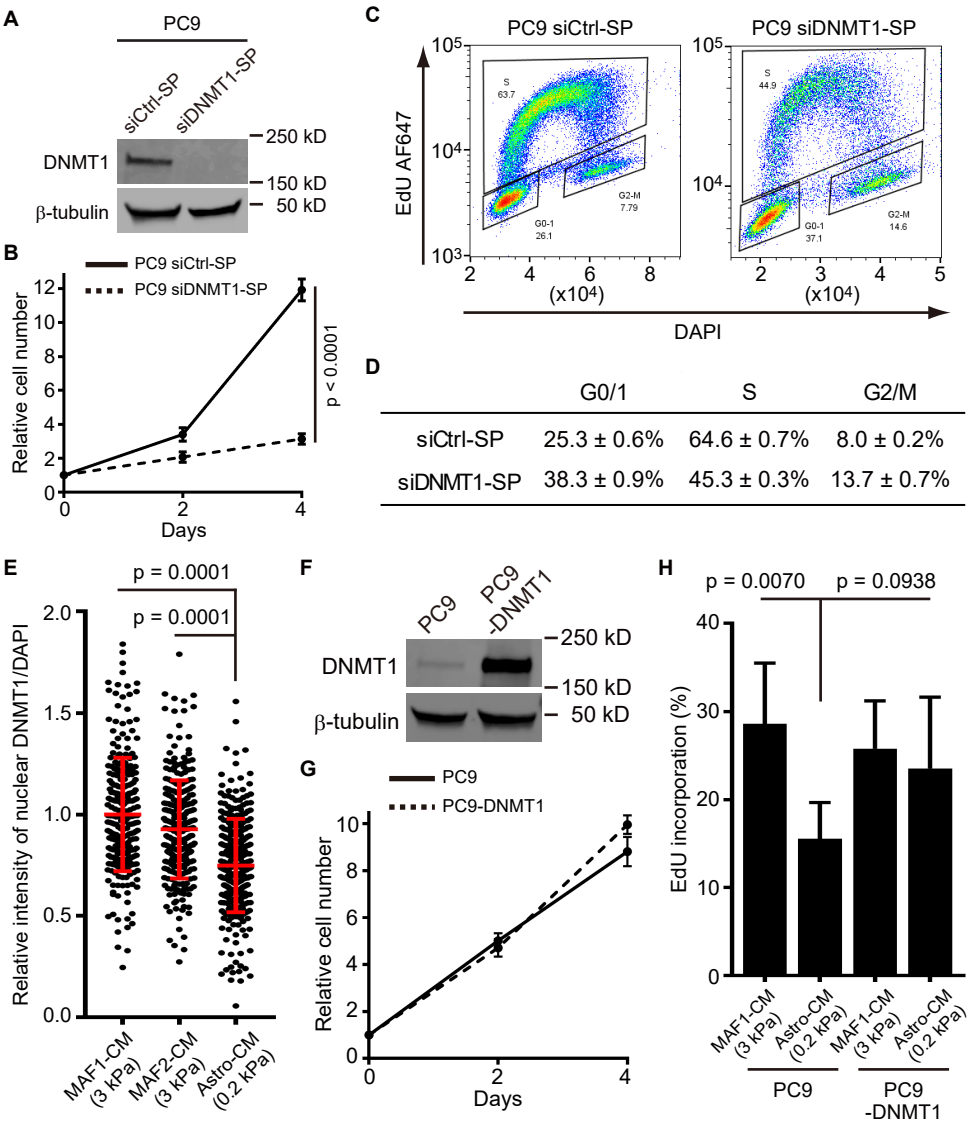

Fig. S5 Hirata et al.

Figure S5 (Related to Figure 3 and 4). DNMT1 suppression induces cell cycle delay in PC9 human lung cancer cells. A, Immunoblotting at day 7 showed effective ablation of DNMT1 in PC9 cells treated with siCtrl smart pool (siCtrl-SP) or siDNMT1 smart pool (siDNMT1-SP). **B**, Cell proliferation analysis of PC9 cells treated with siCtrl-SP or siDNMT1-SP. **C** and **D**, Cell cycle analysis of PC9 cells treated with siCtrl-SP or siDNMT1-SP with EdU incorporation and DAPI staining (n = 3). **E**, DNMT1 expression in PC9 cells cultured in the indicated conditions. Y-axis indicates normalized intensity of DNMT1/DAPI (n = 258-312). **F**, Immunoblotting for DNMT1 in PC9 cells and PC9 cells overexpressing DNMT1 (PC9-DNMT1). **G**, Cell proliferation analysis of PC9 and PC9-DNMT1 cells (n = 3). **H**, EdU incorporation by PC9 and PC9-DNMT1 cells in the indicated culture conditions (n = 6). Data are all mean ± s.d.

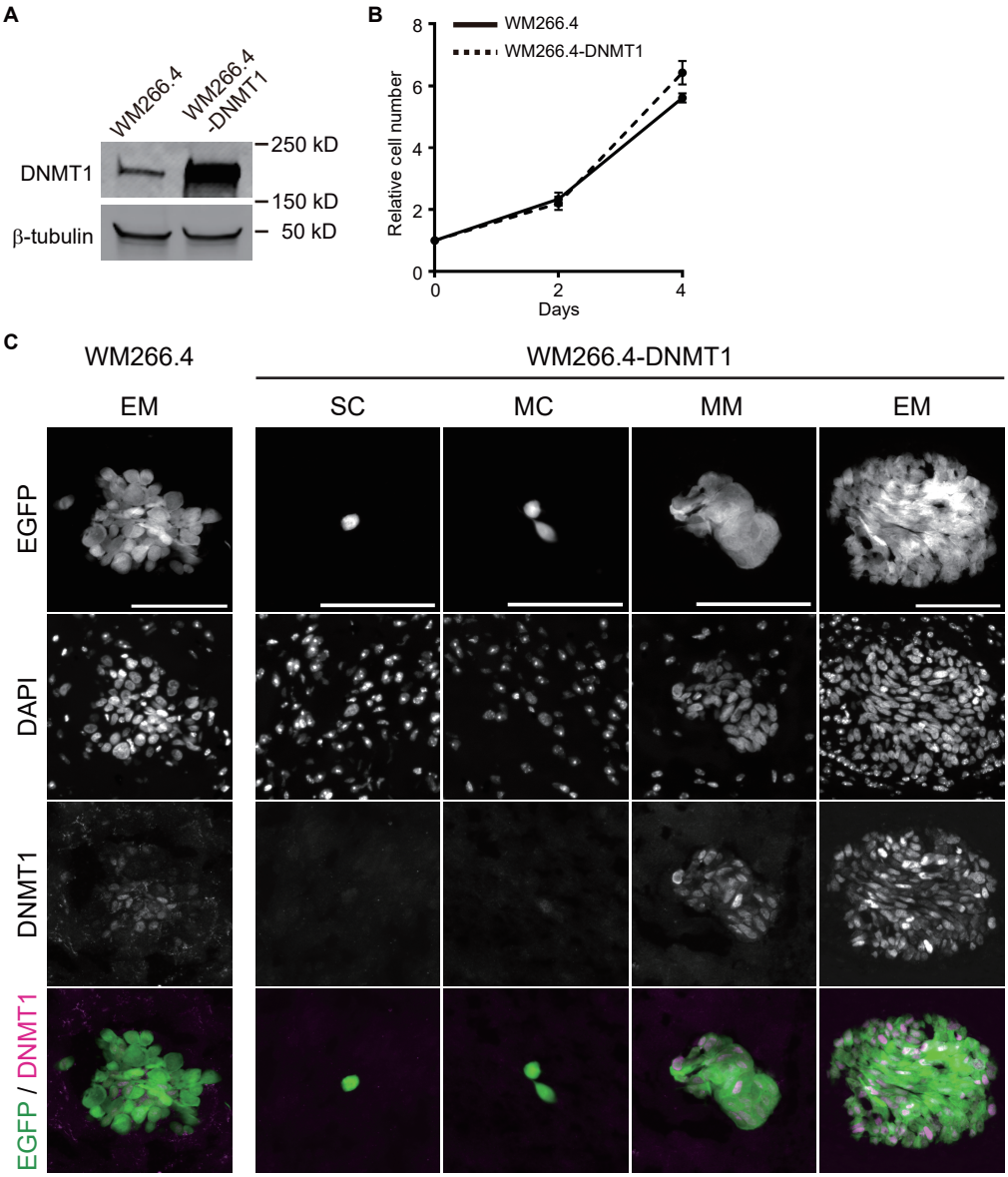

Fig. S6 Hirata et al.

Figure S6 (Related to Figure 4). Indolent brain metastases induced by intra-cardiac injection of DNMT1-overexpressing WM266.4 cells express low levels of DNMT1. A, Immunoblotting for DNMT1 in WM266.4 cells and WM266.4 cells overexpressing DNMT1 (WM266.4-DNMT1). **B**, Cell proliferation analysis of WM266.4 and WM266.4-DNMT1 cells. **C**, Representative images of brain metastatic WM266.4 cells (reference) and WM266.4-DNMT1 cells stained for DNMT1. Green: WM266.4 or WM266.4-DNMT1, Magenta: DNMT1. Scale = 100 μm. Data are all mean ± s.d.

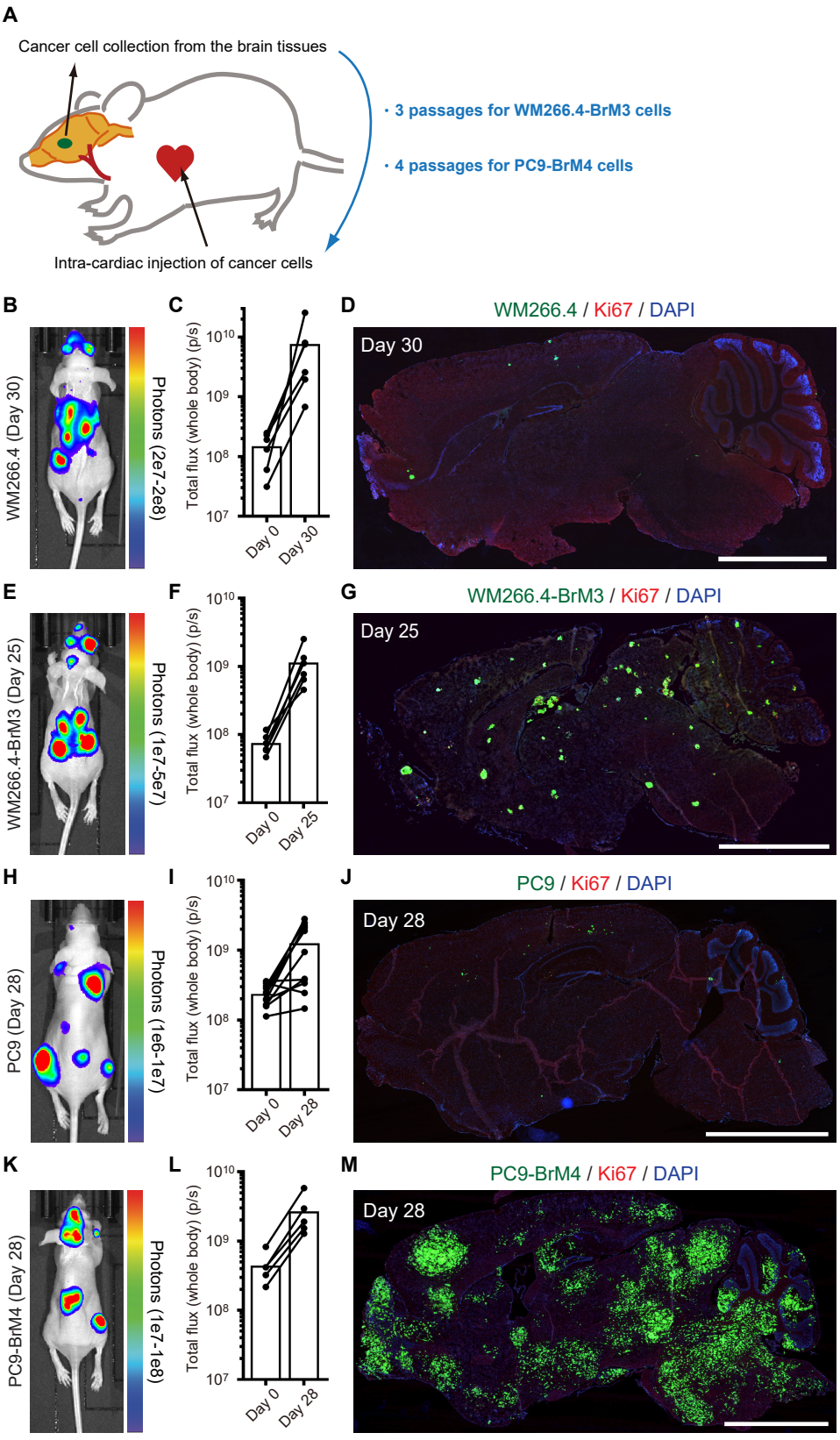

Fig. S7 Hirata et al.

Figure S7 (Related to Figure 5). Characterization of WM266.4 human melanoma cells and PC9 human lung cancer cells with enhanced capability of brain metastasis. A, A scheme of consecutive injection and collection of brain metastatic cancer cells to establish cells with enhanced capability of brain metastasis. **B**-**G**, WM266.4 or WM266.4-BrM3 cells were injected into mouse hearts and induced brain metastasis. Representative images of bioluminescence detection (**B** and **E**), total flux from the whole body (photon/sec) (n = 6 in each group) (**C** and **F**) and representative images of sagittal brain sections stained for Ki67 (**D** and **G**) at the indicated days are shown. Green: WM266.4 or WM266.4-BrM3, Blue: DAPI, Red: Ki67. Scale = 2.5 mm. Note; Both WM266.4 and WM266.4-BrM3 cells metastasize to eye balls and the mice need to be euthanized around 4-5 weeks and 3-4 weeks, respectively. **H**-**M**, PC9 or PC9-BrM4 cells were injected into mouse hearts and induced brain metastasis. Representative images of bioluminescence detection (**H** and **K**), total flux from the whole body (photon/sec) (PC9; n = 11, PC9-BrM4; n = 5) (**I** and **L**) and representative images of sagittal brain sections stained for Ki67 (**J** and **M**) at the indicated days are shown. Green: PC9 or PC9-BrM4, Blue: DAPI, Red: Ki67. Scale = 2.5 mm. Please also refer to Supplementary File S1 for detailed characterization of the mouse models, and Supplementary File S7 and S8 for comparative transcriptome analyses.

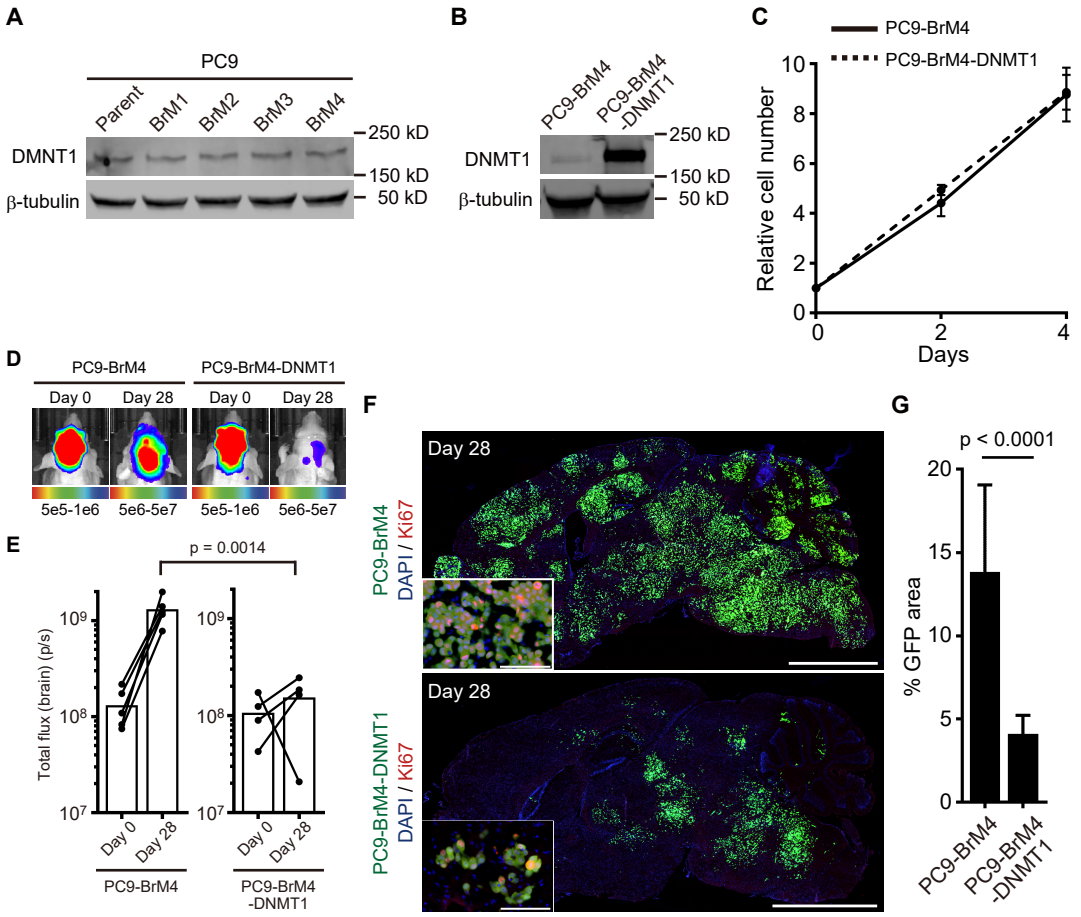

Fig. S8 Hirata et al.

Figure S8 (Related to Figure 5). Forced expression of DNMT1 cancelled the brain tropism of PC9-BrM4 cells. A, Immunoblotting for DNMT1 in PC9 (parent) and its derivatives with enhanced brain tropism (BrM1-4). **B**, Immunoblotting for DNMT1 in PC9-BrM4 cells and PC9-BrM4 cells overexpressing DNMT1 (PC9-BrM4-DNMT1). **C**, Cell proliferation analysis of PC9-BrM4 and PC9-BrM4-DNMT1 cells (n = 3). **D** and **E**, PC9-BrM4 or PC9-BrM4-DNMT1 cells were injected into mouse hearts and induced brain metastasis. Representative images of bioluminescence detection at day 0 (after injection) and day 28 (**D**) and total flux from the brain (photon/sec) (PC9-BrM4; n = 5, PC9-BrM4-DNMT1; n = 4) (**E**) are shown. **F** and **G**, Representative images of sagittal brain sections stained for Ki67 (**F**) and the relative tumor area in the brain sections (% GFP area) at day 28 (**I**) are shown. 10 brain slices from 5 mice (PC9-BrM4) and 8 brain slices from 4 mice (PC9-BrM4-DNMT1) were used for quantification. Green: PC9-BrM4 or PC9-BrM4-DNMT1, Blue: DAPI, Red: Ki67. Scale = 2.5 mm (large images), 100 μm (small panels). Data are mean (**E**) or mean ± s.d (**C** and **G**).

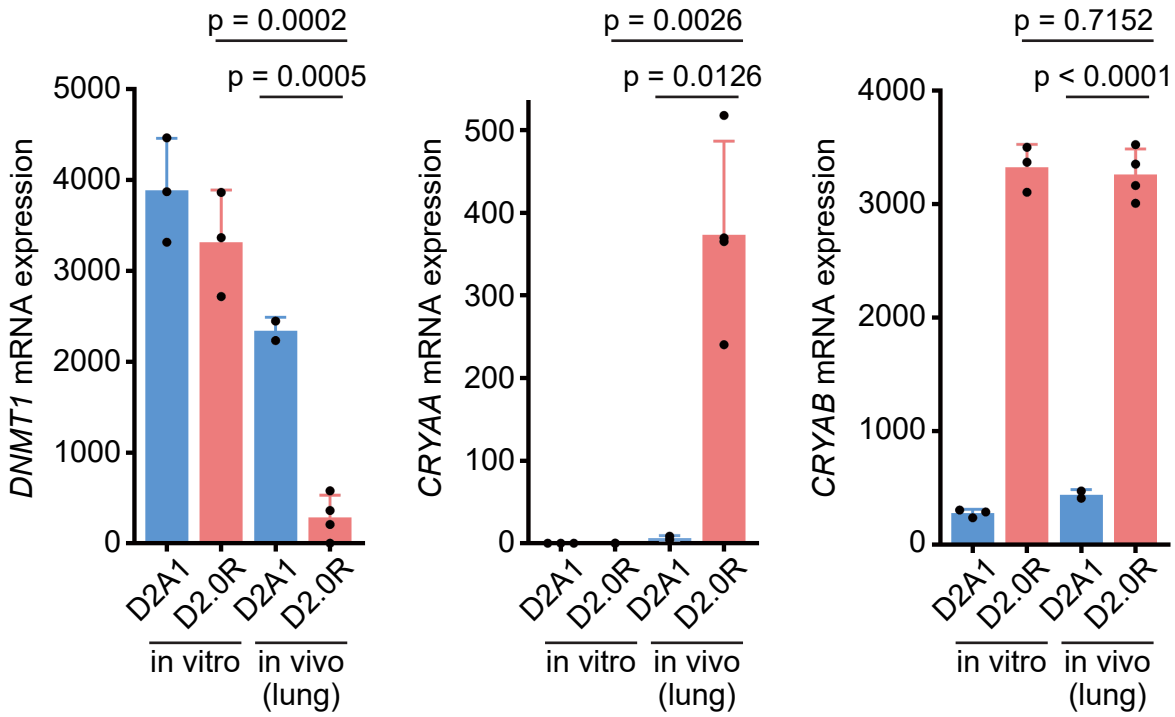

Fig. S9 Hirata et al.

Figure S9 (Related to Figure 6). CRYAA is highly induced in indolent lung-metastatic breast cancer cells. Gene expression analysis of D2A1 and D2.0R mouse breast cancer cells *in vitro* and *in vivo* (lung metastasis). RNA sequencing results are from Montagner et al., Nat Cell Biol. 2020 (GSE120628). Data are all mean ± s.d.

Table S1 (Related to Figure 1). The list of 99 house-keeping genes used in PCA.

Gene_symbol	RefSeq	Gene_symbol	RefSeq	Gene_symbol	RefSeq
ABCF1	NM_001090	HNRNPM	NM_005968	RPL4	NM_000968
ANAPC5	NM_016237	HSP90AB1	NM_007355	RPL6	NM_000970
ARF1	NM_001658	IK	NM_006083	RPL9	NM_000661
ARF3	NM_001659	ILF2	NM_004515	RPS10	NM_001014
ATP6V0B	NM_004047	JTB	NM_006694	RPS11	NM_001015
ATP6V0E1	NM_003945	KARS	NM_005548	RPS13	NM_001017
C11orf58	NM_014267	KAT7	NM_007067	RPS24	NM_001026
C1D	NM_006333	KHDRBS1	NM_006559	RPS25	NM_001028
CANX	NM_001746	KXD1	NM_024069	RPS27A	NM_002954
CAPNS1	NM_001749	NARS	NM_004539	RPS3A	NM_001006
CBX3	NM_016587	NONO	NM_007363	RPS5	NM_001009
CFL1	NM_005507	NPM1	NM_002520	RPS6	NM_001010
CNPPD1	NM_015680	OAZ1	NM_004152	RPS7	NM_001011
COX4I1	NM_001861	PARK7	NM_007262	RTCB	NM_014306
CTDNEP1	NM_015343	PRPF8	NM_006445	SART1	NM_005146
DAD1	NM_001344	PSMB2	NM_002794	SART3	NM_014706
DDX39B	NM_004640	RHOA	NM_001664	SEPT2	NM_004404
DDX5	NM_004396	RNPS1	NM_006711	SLC25A3	NM_002635
EEF2	NM_001961	RPL10A	NM_007104	SMNDC1	NM_005871
EIF3D	NM_003753	RPL11	NM_000975	SNRNP200	NM_014014
EIF3F	NM_003754	RPL12	NM_000976	SNX3	NM_003795
EIF4G2	NM_001418	RPL14	NM_003973	SPAG7	NM_004890
ERH	NM_004450	RPL17	NM_000985	SRP14	NM_003134
FAU	NM_001997	RPL18	NM_000979	SRSF9	NM_003769
FNTA	NM_002027	RPL19	NM_000981	STARD7	NM_020151
GDI2	NM_001494	RPL21	NM_000982	TAF10	NM_006284
GUK1	NM_000858	RPL24	NM_000986	TARDBP	NM_007375
H3F3A	NM_002107	RPL27	NM_000988	TCEB2	NM_007108
HINT1	NM_005340	RPL28	NM_000991	TMED2	NM_006815
HNRNPA1	NM_002136	RPL30	NM_000989	USP22	NM_015276
HNRNPC	NM_004500	RPL34	NM_000995	YY1	NM_003403
HNRNPD	NM_002138	RPL35	NM_007209	ZNF146	NM_007145
HNRNPK	NM_002140	RPL37	NM_000997	ZPR1	NM_003904

TRANSPARENT METHODS

Cells and probes

WM266.4 human melanoma cell line is a gift from late Prof. Chris Marshall (Institute of Cancer Research, London, UK). MDA-MB-231 human breast cancer cell line and PC9 human lung cancer cell line were obtained from the Cell services unit at The Francis Crick Institute and RIKEN Cell Bank, respectively. Mouse primary astrocytes and microglial cells were established from euthanized neonatal C57BL6 mice (P1-3, male and female) by using gentleMACS Dissociator and MACS Cell Separation system with anti-ACSA2 antibody and anti-CD11b antibody, respectively (Miltenyi Biotec). The origins of human melanoma-associated fibroblasts (MAF1, MAF2) are described previously (Hirata et al., 2015). All the cells were maintained in DMEM with 10% FBS / 1% PenStrep (GIBCO), except that primary astrocytes were cultured in Astrocyte Medium (ScienCell) during establishment period. All the constructs (EGFP, mCherry, firefly luciferase, human DNMT1) were cloned into pBabe or pCX4 retrovirus vector (Akagi et al., 2003) and introduced into the cells. pLenti-U6-sgRNA-SFFV-cas9-2A-Puro was obtained from abm for αB-crystallin knock out with the target sequence; GTGGATGGCGATGTCCATG.

Mouse models, tissue preparation, immunohistochemistry, image acquisition and data analysis

Animal experiments were done in accordance with UK regulations under project license PPL/80/2368, the Institutional Animal Care and Use Committee of Kanazawa Medical University (2018-27) and the Institute for Experimental Animals of Kanazawa University (AP-184026). For systemic/brain metastasis models, cancer cells stably expressing a fluorescent protein (mEGFP or mCherry) and firefly luciferase (1 x 10^6 cells/200 μl PBS in total) were injected into the left ventricle of anesthetized 8-weeks-old female nude mice (Balb/c nu/nu). Successful injection was confirmed by intraperitoneal

injection of D-Luciferin (150 mg/kg) and bioluminescence imaging (BLI) with IVIS Spectrum or IVIS LuminaXRMS (PerkinElmer). Progression of systemic metastasis was confirmed by follow up BLI and mice were euthanized at proper day for further analysis. For ex vivo BLI, mouse brains were surgically extracted after *in vivo* BLI, cultured in D-Luciferin-containing PBS (0.3 mg/ml) and imaged with IVIS XRMS. For histopathological analysis, mouse brains were fixed with 10% NBF or Mildform (WAKO) and frozen in O.C.T compound (Sakura Finetek). A tissue slice of 10 μm thickness was prepared with Cryostat (Leica) and mounted on silane-coated glass slides. We prepared serial sections from the center of the brain hemispheres and included both sides for immunostaining and quantification. The brain slices were blocked with 5% BSA and 1% FBS in PBS and incubated overnight with the primary antibodies listed in the last section of this Supplementary Information. On the next day, the samples were washed with PBS and incubated with secondary antibodies (also listed in the last section of this Supplementary Information) for 2 hours at room temperature. After washing with PBS, the samples were covered with VECTASHIELD with DAPI (Vector Laboratories), and the slides were scanned with NanoZoomer (Hamamatsu Photonics) or IX83 inverted microscope (Olympus). Acquired images were analyzed with MetaMorph software (Universal Imaging). The number of metastatic lesions were counted manually, and the relative tumor area (% GFP area) was calculated semi-automatically. For the quantification of Ki67-index (Fig. 1E and 1F) and DNMT1-positive ratio (Fig. 2F), cells with higher nuclear Ki67 or DNMT1 intensity than the background staining were manually counted as positive on 24-bit ndpi image files (Hamamatsu Photonics), and we objectively analyzed 117 lesions (MM at day 20), 64 lesions (EM at day 20), 123 lesions (MM at day 30) and 82 lesions (EM at day 30) for Ki67-index and 37 lesions (SC at day 30), 32 lesions (MC at day 30), 39 lesions (MM at day 30) and 21 lesions (EM at day 30) for DNMT1-positive ratio. For the quantification of normalized intensity of DNMT1/DAPI *in vivo* (Supplementary Fig. S2B), six EM lesions at day 30 were imaged

with IX83 inverted microscope and analyzed with background-subtracted 14-bit grayscale images. Regarding the number of brain slices we used for quantification, we used 28-32 slices in the first analysis (Fig. 1), but later we found that we could obtain equivalent results with smaller number of sections (6-12 slices). In the case of DNMT1 overexpression, we analyzed additional number of slices (20-24 slices) because we obtained unexpected results that induction of DNMT1 reduced the number of brain metastatic lesions.

Establishment of cancer cell lines with enhanced capability of brain metastasis

Cancer cells with enhanced brain tropism were established as described elsewhere (Bos et al., 2009). Briefly, WM266.4 human melanoma cells or PC9 human lung cancer cells expressing EGFP and firefly luciferase were injected into the left ventricle of anesthetized nude mice. The mouse brains were cut out ~33 days after intra-cardiac injection and dissociated into single cells by using gentleMACS Dissociator (Miltenyi Biotec). The dispersed cells were cultured on a plastic dish with appropriate antibiotics to select cancer cells and BrM1 cells were established. BrM2, BrM3 and BrM4 cells were established by the repetition of the intra-cardiac injection and cancer cell collection.

Collection of brain metastatic cancer cells and single cell RNA sequencing

Mouse brain was cut out 20 days after intra-cardiac injection of WM266.4-Luc-EGFP cells or WM266.4-Luc-EGFP cells pre-labeled with CellVue Claret Far Red (Sigma-Aldrich), and dissociated into single cells by using gentleMACS Dissociator (Miltenyi Biotec). The dispersed cells were seeded onto a plastic dish and cultured for 1 hours, then the cells attached on the bottom of the plate were collected. We successfully analyzed 3,077 EGFP-positive cells (WM266.4-Luc-mEGFP cells) from 6 mice to detect CellVue Claret Far Red-positive cells with ASONE Cell Picking System (ASONE), and successfully collected about 3,000 EGFP-positive cells (the estimated number of the cells

by microscopic analysis was 3,094) from 6 mice for single cell RNA sequencing. The cells were applied to the C1 Single-Cell Auto Prep System (Fluidigm) and confirmed that the Fluidigm C1 ICF contains a single WM266.4 cell by real-time imaging with its size and appearance. Then, we underwent on-chip RNA preparation and whole-transcriptome amplification with SMART-Seq v4 Ultra kit for 96 individual cells. The products were then converted to Illumina sequencing libraries using Nextera XT (Illumina) and was subjected to next-generation sequencing from both ends with the HiSeq 2500 platform (Illumina). For expression profiling with RNAseq data, paired-end reads were aligned to the human genome assembly (hg19) using the TopHat2 (https://ccb.jhu.edu/software/tophat/index.shtml). Fragments Per Kilobase Million (FPKM) values for each gene were calculated from mapped read counts using Cuffquant and normalized with the Cuffnorm (http://cole-trapnell-lab.github.io/cufflinks/). We confirmed that all the cDNA libraries were effectively mapped on hg19 human genome assembly, indicating that all the analyzed cells were WM266.4 cells. To removing the outlier cells, principal component analysis (PCA) was perfomed with FPKM values of 99 house keeping genes (provided in Supplementary Table S1). Futher PCA was done to classify the remaining 61 cells using FPKM of CELL_CYCLE_PROCESS gene set of MsigDB (http://software.broadinstitute.org/gsea/index.jsp).

Gene set enrichment analysis

Single cell RNAseq data was processed and analysed using the Gene-set enrichment analysis software following the program guidelines (Subramanian et al., 2005). Values in the tables represent normalized enrichment score (NES), nominal p-value and false discovery rate q-value of each gene set. Details of all gene sets used are available at the Broad Institute website (http://software.broadinstitute.org/gsea/index.jsp)

RNAseq library construction and data analysis

Total RNA was extracted using the RNeasy Mini Kit (Qiagen) and the integrity was examined with the TapeStation (Agilent Technologies). cDNA was prepared from polyA-selected RNA by using an NEBNext Ultra Directional RNA Library Prep kit (New England BioLabs) and was subjected to next-generation sequencing from both ends with the HiSeq 2500 platform (Illumina). For expression profiling, paired-end reads were aligned to the human genome assembly (hg19) using the TopHat2. FPKM for each genes were calculated and normalized with Cufflinks pipeline. Genes of which average expression levels are in the top 20% in siDNMT1-treated cells (FPKM > 13.44) and upregulated > 1.5 fold compared with siCtrl treated cells with p-value < 0.0001 were considered to be suppressed by DNMT1.

Immunocytofluorescence

Cultured cells were fixed with 4% paraformaldehyde in PBS, permeabilized with 0.4% Triton X-100 in PBS, blocked with 5% BSA and 1% FBS in PBS and incubated overnight with the primary antibodies listed in the last section of this Supplementary Information. On the next day, the cells were washed with PBS and incubated with secondary antibodies (also listed in the last section of this Supplementary Information) for 1 hour at room temperature. After rising in PBS, the cells were stained with DAPI and imaged with IX83 inverted microscope (Olympus). Acquired images were analyzed with MetaMorph software (Universal Imaging) and signal intensities in nuclei were calculated semi-automatically.

Cell culture on PAA/Bis-AA gels with defined stiffness

PAA/Bis-AA gels with defined stiffness were set up on glass bottom dishes as reported previously (Hirata et al., 2015). Briefly, 25 μl of PAA/Bis-AA solution (the composition provided below) was put on a glass bottom dish, covered with a cover glass with 18 mm in diameter and left for 1 hr at RT to set a gel with about 100 μm in

thickness. After removing the cover glass, the gel was coated with 200 μl of Sulfo-SANPAH photoreactive crosslinker (ThermoFisher Scientific) and activated by UV illumination for 10 min, followed by coating with 50 mg/ml fibronection overnight. The next day, cells were seeded onto the gel ($2x10^4$ cells in 200 μl DMEM) and cultured for up to 4 hours. Once the cells were found to adhere on the gel, the media were changed to the conditioned media. To obtain conditioned media, 60-80% confluent astrocytes, microglial cells or fibroblasts were incubated for 48 h in DMEM with 10% FBS / 1% PenStrep, and then supernatants were collected. The cells were cultured for 5 days by changing the media every two days and sent for the following experiments. Composition of the gels are described below.

Composition of PAA/Bis-AA gels		
Young's modulus	**0.2 kPa**	**3 kPa**
10mM HEPES	424.7 μl	403 μl
40% PAA	37.5 μl	68.6 μl
2% Bis-AA	7.5 μl	22.48 μl
APS	2.5 μl	2.5 μl
TEMED	0.25 μl	0.25 μl
(Fibronectin coating)	(50 mg/ml)	(50 mg/ml)

Cell proliferation assay

1 x 10^5 cells in DMEM with 10% FBS were seeded onto 6-well plate (2 ml) and the numbers of the cells were counted by using Countess II Automated Cell Counter (Thermo Fisher Scientific) on the indicated days. For MTS assay, 5,000 cells in DMEM with 10% FBS were seeded onto 96-well plate (100 μl) and relative cell numbers were calculated with CellTiter 96® Aqueous One Solution (Promega Corporation) following the manufacture's instruction. Media were changed every two days. For *in vitro*

bioluminescence imaging, 5,000 cells stably expressing firefly luciferase were seeded onto 96-well plate (100 μl) and relative cell numbers were calculated with IVIS LuminaXRMS.

siRNA transfection

Cells were prepared on 6-well plate the day before, and control siRNA (ON-TARGET plus Non-targeting Pool, Dharmacon) or siRNA against DNMT1 (ON-TARGET plus Human DNMT1 siRNA SMARTpool, Dharmacon) were transfected with lipofectamine RNAiMax (Invitorgen) according to the manufacture's protocol on day 0. The cells were subcultured to 9 cm dish on day 2 and siRNAs were transfected again on day 3. The cells were further expanded and sent for the following experiments on day 7. The siRNA sequences are provided below.

siRNA		
	Company	**Sequence**
Non-targeting Pool	Dharmacon	#1 GAACGGAUUUGAUGAAUGA #2 CCACAGAAGUUUACAUUAA #3 GCACAGAUCCCAAGUUUCA #4 CAAGAGGGCUGAAGAUUAC
Human DNMT1 siRNA SMARTpool	Dharmacon	#1 GAACAUGGCCGACCUGAUU #2 GAAGUUGGGUUGUUUGGAA #3 GAAGAUAAGCCAACAUUGA #4 AGAUGUUGGUUUAAAGCGA

Cell cycle analysis

EdU incorporation assay was performed by using Click-iT Plus EdU Flow Cytometry Assay Kits or Click-iT Plus EdU Imaging Kits (ThermoFisher Scientific) following the manufacture's protocol. Briefly, cancer cells transfected with control siRNAs or cultured on PAA/Bis-AA gels were incubated with 10 μM EdU for 1 hour. For flow cytometry

analysis, the cells were trypsinized, fixed with 4% PFA, permeabilized and labeled with Alexa Fluor 647 picolyl azide. Then, the cells were stained with DAPI and analyzed with Cell Sorter SH800 (Sony). For imaging analysis, the cells on the gels were directly fixed with 4% PFA, permeabilized and labeled with Alexa Fluor 555 picolyl azide. Then, the cells were stained with DAPI and imaged under epifluorescent microscope (IX83, Olympus).

RNA extraction and real-time PCR.

Total RNA was extracted by using TRIZOL reagent (Thermo Fisher Scientific) following the manufacture's protocol. cDNA was synthesized with oligo-dT primer by using SuperScript III Reverse Transcriptase (Thermo Fisher Scientific), and real-time PCR was performed by using THUNDERBIRD SYBR qPCR Mix (TOYOBO) and Mx3000P qPCR System (Agilent). Relative expression of each gene was normalized by GAPDH expression. The primer sequences are listed below.

Target gene	Forward	Reverse
DNMT1	CCACCACCAAGCTGGTCTACC	AACCATGTCCTTGCAGGCTT
CRYAB	GTCAACCTGGATGTGAAGCA	GTGGAACTCCCTGGAGATGA
L1CAM	ATGGTACAGTCTGGGCAAGG	CGGGGCCATATTTGTTTATG
SERPIND1	CTCACCAAGGGCCTCATAAA	TCTCTCATTCAGCCGGAAGT
SERPINE2	CTTTGAGGATCCAGCCTCTG	TACACTGCGTTGACGAGGAC
GAPDH	AAATCCCATCACCATCTTCCA	AATGAGCCCCAGCCTTCTC

DNA methylation analysis

Genomic DNAs from cancer cells were extracted with NucleoSpin Tissue kit (Macherey-Nagel). Two μg of DNA was treated with bisulfite using an EpiTect Plus Bisulfite kit (Qiagen). DNA methylation status was analyzed by pyrosequencing technology (PyroMark Q24, Qiagen) (Goto et al., 2009). PCR primers for

pyrosequencing were designed by Pyromark Assay Design 2.0 (Qiagen) and provided below. *LINE-1* is used as a marker of global DNA methylation (average of three CpG sites: ttCGtggtgCGtCGttt) and *EBF3* as a representative highly-methylated region in melanoma cells (Chatterjee et al., 2017). The methylation of *L1CAM* is the average of five CpG sites in the promoter region (CGcaggagcCGgtgctcCGCGgCG).

Target gene	Forward	Reverse	Sequencing
LINE-1	TTTTGAGTTAGGTGTGGGATATA	AAAATCAAAAAATTCCCTTTC	AGTTAGGTGTGGGATATAGT
EBF3	GGGACACCGCTGATCGTTTAGTTTTGTAGTAGTTTTAGGTTTGTTTAGA	ACACAATTACAATTTAACCCCTTAATAC	CRAAAAAAAAATAAAAAAAAACAAATC
L1CAM	GGGAAAGGTYGAATGGGGTTAAT	GGGACACCGCTGATCGTTTACCTAAAAACCCAATCAAAATCCTATTAA	TTGGGTTTTGGGGTG

Immunoblotting

Protein lysates were processed following standard procedures and analyzed by SDS-PAGE followed by immunoblotting. Precast SDS-polyacrylamide gels (4‑15% Mini-PROTEAN TGX Precast Gel) and Trans-Blot Turbo transfer system were purchased from BioRad and bound antibodies were detected with secondary antibodies conjugated with IRDye680 or IRDye800 and analyzed with an Odyssey Imager system (LICOR). Antibody description and working dilutions can be found in the last section of this Supplementary Information.

Primary antibodies

Target	Company	Cat. No	Dilution		
			IF	WB	IHC
Ki67	Abcam	ab15580	1 μg/ml		
Ki67	Invitrogen	14-5698-82	5 μg/ml		
DNMT1	Abcam	ab188453	1:1000	1:1000	

αB-crystallin	Abcam	ab76467	1:250	1:1000	
GFAP	Abcam	ab7260			1:1000
Iba-1	WAKO	019-19741	1:1000		
β-tubulin	Sigma	T7816		1:20000	

Secondary antibodies

1. Goat anti-Rabbit IgG (H+L) Highly Cross-Adsorbed Secondary Antibody, Alexa Fluor Plus 555 (ThermoFisher, A-32732) 1:500
2. Goat anti-Rat IgG (H+L) Cross-Adsorbed Secondary Antibody, Alexa Fluor 647 (ThermoFisher, A-21247) 1:500
3. IRDye® 680RD Donkey-anti-Rabbit Antibody (LI-COR, 926-68073) 1:10,000
4. IRDye® 800 Donkey Anti-Mouse IgG (H+L) (LI-COR, 926-32212) 1:10,000

Statistical analysis

Data were subjected to one-way ANOVA analysis, followed by Dunnett's multiple comparison test. When two groups were compared, a two-tailed paired or unpaired Student's t-test was applied.

SUPPLEMENTAL REFERENCE

Akagi, T., Sasai, K., and Hanafusa, H. (2003). Refractory nature of normal human diploid fibroblasts with respect to oncogene-mediated transformation. Proceedings of the National Academy of Sciences of the United States of America *100*, 13567-13572.

Bos, P.D., Zhang, X.H., Nadal, C., Shu, W., Gomis, R.R., Nguyen, D.X., Minn, A.J., van de Vijver, M.J., Gerald, W.L., Foekens, J.A.*, et al.* (2009). Genes that mediate breast cancer metastasis to the brain. Nature *459*, 1005-1009.

Chatterjee, A., Stockwell, P.A., Ahn, A., Rodger, E.J., Leichter, A.L., and Eccles, M.R. (2017). Genome-wide methylation sequencing of paired primary and metastatic cell lines identifies common DNA methylation changes and a role for EBF3 as a candidate

epigenetic driver of melanoma metastasis. Oncotarget *8*, 6085-6101.

Goto, Y., Shinjo, K., Kondo, Y., Shen, L., Toyota, M., Suzuki, H., Gao, W., An, B., Fujii, M., Murakami, H.*, et al.* (2009). Epigenetic profiles distinguish malignant pleural mesothelioma from lung adenocarcinoma. Cancer research *69*, 9073-9082.

Hirata, E., Girotti, M.R., Viros, A., Hooper, S., Spencer-Dene, B., Matsuda, M., Larkin, J., Marais, R., and Sahai, E. (2015). Intravital imaging reveals how BRAF inhibition generates drug-tolerant microenvironments with high integrin beta1/FAK signaling. Cancer cell *27*, 574-588.

Subramanian, A., Tamayo, P., Mootha, V.K., Mukherjee, S., Ebert, B.L., Gillette, M.A., Paulovich, A., Pomeroy, S.L., Golub, T.R., Lander, E.S.*, et al.* (2005). Gene set enrichment analysis: a knowledge-based approach for interpreting genome-wide expression profiles. Proceedings of the National Academy of Sciences of the United States of America *102*, 15545-15550.